



EXPERIMENTAL AND NUMERICAL INVESTIGATION OF AXIAL FAN AEROACOUSTICS AT DISTURBED INFLOW CONDITIONS

Andreas LUCIUS¹, Simon HÜTTER¹, Philipp DIETRICH¹,
Marc SCHNEIDER¹, Marius LEHMANN¹, Thomas GEYER²

¹ *ebm-papst Mulfingen GmbH & Co. KG, Bachmühle 2,
74673 Mulfingen, Germany*

² *Brandenburg University of Technology Cottbus, Chair of Technical
Acoustics, Siemens-Halske-Ring 14, 03046 Cottbus, Germany*

SUMMARY

In the present paper the influence of inflow disturbance on the aeroacoustic performance of an axial fan is investigated numerically and experimentally. Two inflow conditions are considered: the clean inflow condition and the disturbed case with a rectangular box mounted on the suction side. The simulations show large scale vortical structures near bottom and top of the box, which interact with the blades. The location of these vortices corresponds to sound source localisation via microphone array measurements. For both cases the CAA simulation result for far field acoustics are in close agreement to the measurements. Finally the presence of the large scale flow features is proved experimentally via flow visualisation on the box surface.

INTRODUCTION

In customer applications the fan always operates at more or less disturbed inflow conditions. A typical configuration is a fan sucking air through a heat exchanger. When the air flows through the heat exchanger turbulence is generated due to separation of the flow at the tube bundles. The turbulence is desired in terms of increased heat transfer in the heat exchanger. On the other hand the

noise emission of the fan may dramatically rise in comparison to clean inflow conditions. Turbulence ingestion noise is one of the key sound generation mechanisms for airfoils in fluid flow [1]. In a recent study Zenger et al. [2] analysed experimentally the influence of grid induced turbulence on axial fans with different blade sweep. The inflow turbulence was generated with different grids with bar sizes of 4, 12 and 16 mm and solidity kept constant. The measured mean turbulence intensity was in the range of 5 % (no grid) to 20 % (16 mm grid). At design flow rate the increase in overall sound power level with highest turbulence was 6.7 dB for the unskewed fan, 5.4 dB for the backward skewed fan and 9.4 dB for forward skewed fan.

At ebm-papst a simple rectangular box mounted on the fan suction side is used as one reference case for investigation of disturbed inflow conditions (Figure 1). This configuration has only minor influence on fan performance, but strong increase in tonal as well as broad band noise emission of the fan. The aim of the present investigation is to analyse the sound generation mechanisms with the help of microphone array measurements as well as CFD and CAA simulations.

INVESTIGATED FAN CONFIGURATION

In this study two fan configurations were analysed at ebm-papst test rig conditions: the undisturbed fan and the fan with rectangular box. The 5 bladed fan has a diameter of 952 mm operating at 925 rpm. The fan is mounted with a support ring without guard grill. Fan performance and acoustic measurements were conducted simultaneously in the ebm-papst anechoic test rig with reflecting bottom. The test rig allows standardised measurements according to ISO 5801 [3]. The performance curves are shown in non-dimensional form.

$$\psi_{ts} = \frac{2\Delta p_{ts}}{u_2^2} \quad (1)$$

$$\phi = \frac{4Q_v}{\pi D_2 u_2} \quad (2)$$

With the given setup shaft torque is not measured, only the overall total to static efficiency based on electric input power is measured. The measurement uncertainty is 1.0 % for flow rate and 0.5 % for pressure rise. For aeroacoustic measurements the uncertainty is 1 dB for $f > 100$ Hz.



Figure 1: investigated fan configuration: fan in box with microphone array

The acoustic measurements consist of sound pressure measurements on axis of rotation at 1 m (suction side) and 3 m (pressure side) distance to the chamber wall. Sound power is measured with

10 microphones on both sides spanning rectangular enveloping surfaces according to ISO 13347-3 [4]. The signal is recorded for 30 seconds, for the narrow band FFT 16384 points per block are used resulting in frequency resolution of 4 Hz. Figure 2 displays the performance curves of the fan with and without box. The results clearly show that the inflow disturbance in terms of the box has negligible effect on fan performance. The installation effect in this case is entirely aeroacoustic. Total A-weighted sound power increases by 8 dB in the considered operational point at ϕ 0.21. The main increase is in low frequency broad band noise in range of 100 to 1000 Hz. At higher frequencies up to 2 kHz the increase is still 6 dB. Above 2.5 kHz the increase reduces to values around 2 dB.

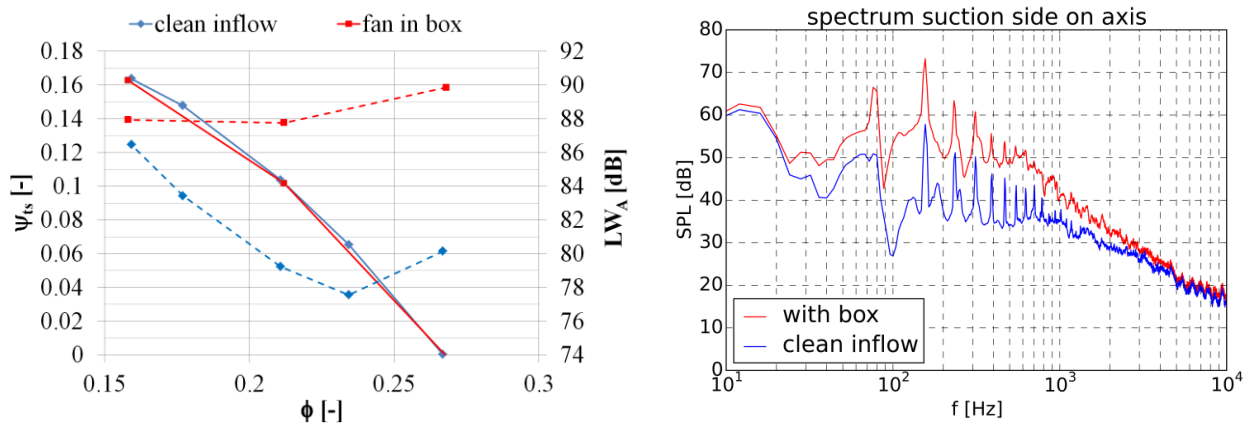


Figure 2: experimental results: (left) performance curves aerodynamics and aeroacoustics, (right) narrow band sound pressure spectrum, suction side on axis

The narrow band spectrum shows, that the increase is in broad band noise as well as tonal noise (blade pass frequency BPF = 77 Hz). The increase in tonal noise suggests that steady flow patterns exist. The blades rotate through this non-uniform flow field leading to interaction with BPF. The sound generation mechanisms were analysed in detail with the help of microphone array technique and numerical simulations.

SOUND SOURCE LOCALISATION WITH MICROPHONE ARRAY

For analysis of sound sources on the rotating blades a microphone array circular rings was applied in the measurements (figure 1). It contains in total 80 microphones on 3 rings. The array was built up in cooperation the Chair of Technical Acoustics of the Brandenburg University of Technology in Cottbus. The software virtually rotates the microphones for localisation in rotating frame of reference. Details on the method demonstrated on a simple open cooling fan are published in the paper of Herold and Sarradj [5]. The rotating array method was successfully applied to axial forward and backward skewed fans by Zenger et al. [6]. Especially for the forward skewed fan the sources move to the leading edge in case of turbulent inflow. This effect was observed for frequencies up to 4 kHz. The software contains several beamforming algorithms, results here were obtained using CLEAN SC [7].

The evaluation of the array was first done in rotating frame of reference. Figure 3 shows the sound maps for frequencies of 1 and 2 kHz, comparing the undisturbed fan with the box installation. For the undisturbed fan at 1 kHz sources are localised in the middle of the blade at outer radial positions. At 2 kHz the sources are found near the trailing edge and in the tip region. This

corresponds to the typical noise source mechanisms trailing edge noise and noise due to the tip vortex. In case of inflow disturbance the sound sources move to the outer radial part of leading edge. At 2 kHz some additional minor sources are found near the trailing edge, but only at large radial positions.

Since the increase of tonal noise in case of fan in box suggests steady flow features beamforming was also applied in steady mode without virtual rotation of the microphones. The resulting sound maps are shown in figure 4. It is interesting to see non rotating sources near middle of the box walls. Sources on bottom and top wall are of higher intensity. Due to the rectangular shape of the box bottom and top walls are closer to the fan.

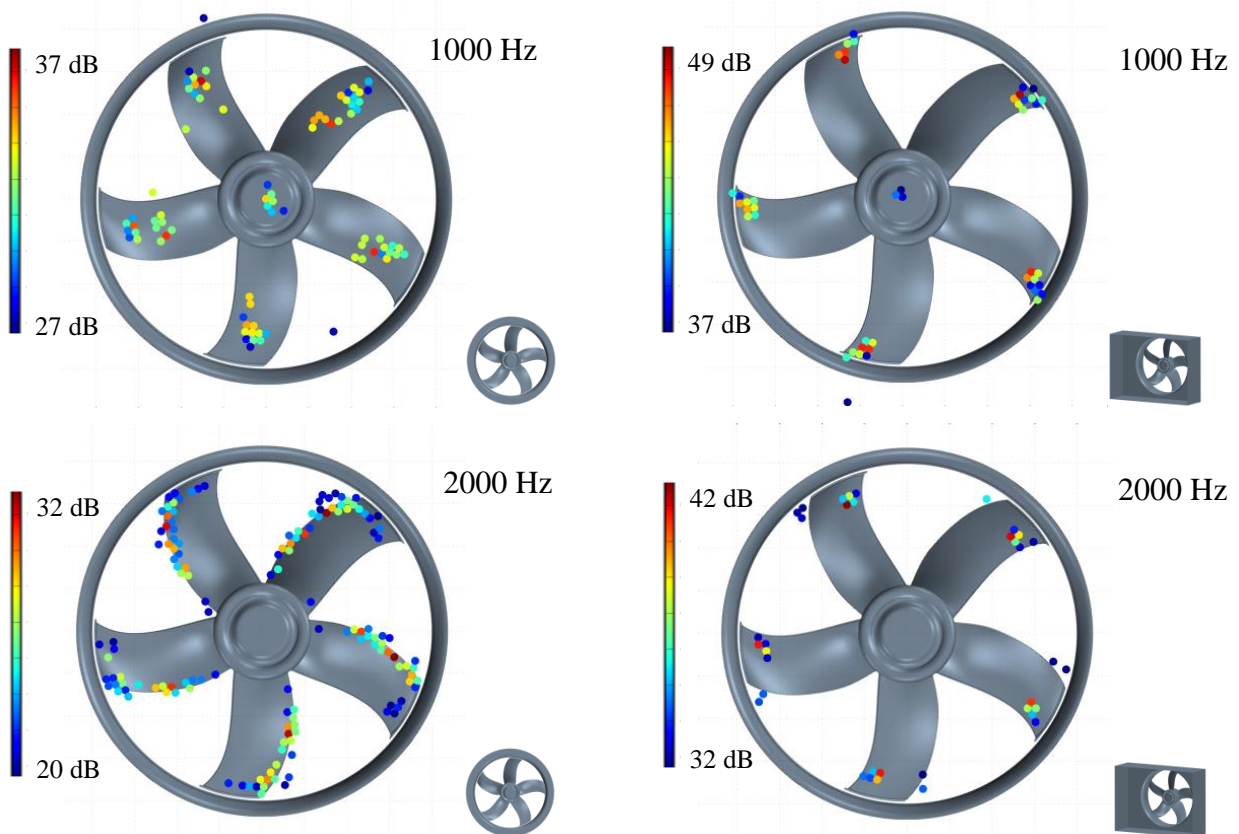


Figure 3: experimental beamforming results,
(top) 1000 Hz, (bottom) 2000 Hz, (left) clean inflow, (right) fan in box

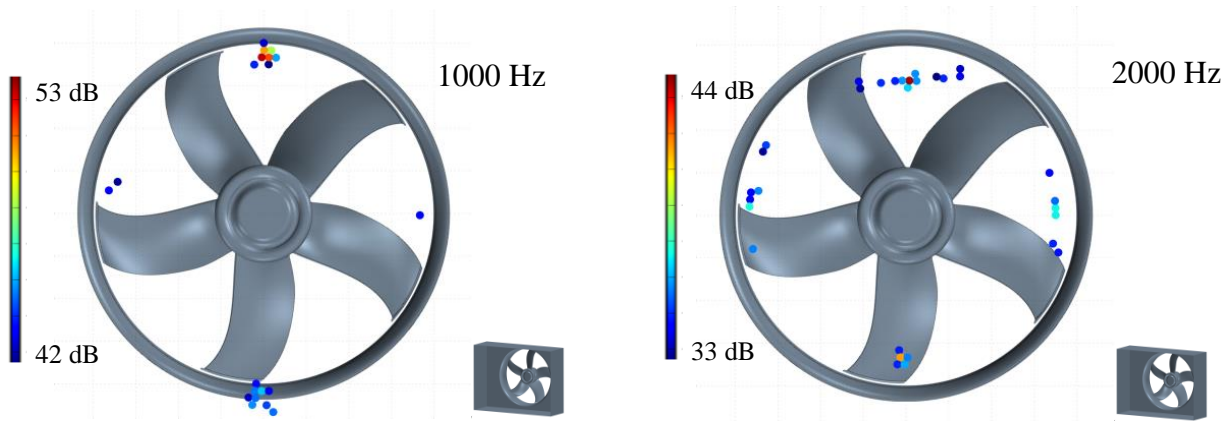


Figure 4: experimental beamforming results, (left) 1000 Hz, (right) 2000 Hz, fan in box, absolute frame of reference

SIMULATION METHOD AND RESULTS

All simulation results presented in this paper were obtained with the general purpose CFD code starCCM+ version 11.02-r8 (double precision). In preliminary studies the influence of grid and simulation setup was analysed with RANS simulations. Finally compressible LES with mesh motion was used to compute the aeroacoustic sources. For the LES the WALE subgrid model was applied. All simulations were done using the segregated solver.

An unstructured polyhedral mesh was used with prism layers to resolve the turbulent boundary layer. The number of cells is given in table 1. The mesh was designed to keep y^+ values below 1 on all solid walls. For LES not only the wall normal but also the tangential resolution needs to be fine enough. Literature suggests for plane boundary layers x^+ (main flow direction) 50...100 as well as z^+ ca. 20 [8]. Within the limits of industrial feasibility x^+ values around 200 were achieved. The under resolved boundary layer leads to under estimation of wall shear stresses compared to RANS reference solutions. Nevertheless the LES achieves a proper prediction of sound spectra.

For the discretisation of the convective terms a 3rd order MUSCL scheme is used. The conservative scheme blends 3rd order upwind with central differences. To keep numerical dissipation as low as possible the blending should be low [9], a value of 0.1 was used.

For temporal discretization 6000 steps per revolution were chosen, leading to a time step of $\sim 1.1e-5$ s. To achieve convergence in each time step 5 inner iterations were used with under relaxation of 0.8 for velocity and 0.6 for pressure.

Table 1: cell count CAA simulations

setup	Cells rotor region [10^6]	Total cells [10^6]
Undisturbed	32.1	46.4
Fan in box	44.2	74.6

Far field sound pressure is derived from the solution of the FW-H equation in formulation of Brentner and Farasat [10]. For the FW-H integral two different emission surfaces were used: an impermeable emission surface (rotating blades) and a permeable surface on the suction side of the

fan marked in yellow in figure 6. The permeable FW-H surface enables the inclusion of installation effects, e.g. reflection of sound waves on the housing or the box. For propagation of sound waves in standard CFD codes 20 cells per wave length are suggested [9]. The mesh resolution in the near field propagation zone is chosen to match this criterion up to 3 kHz. Figure 6 shows the model setup with dimensions.

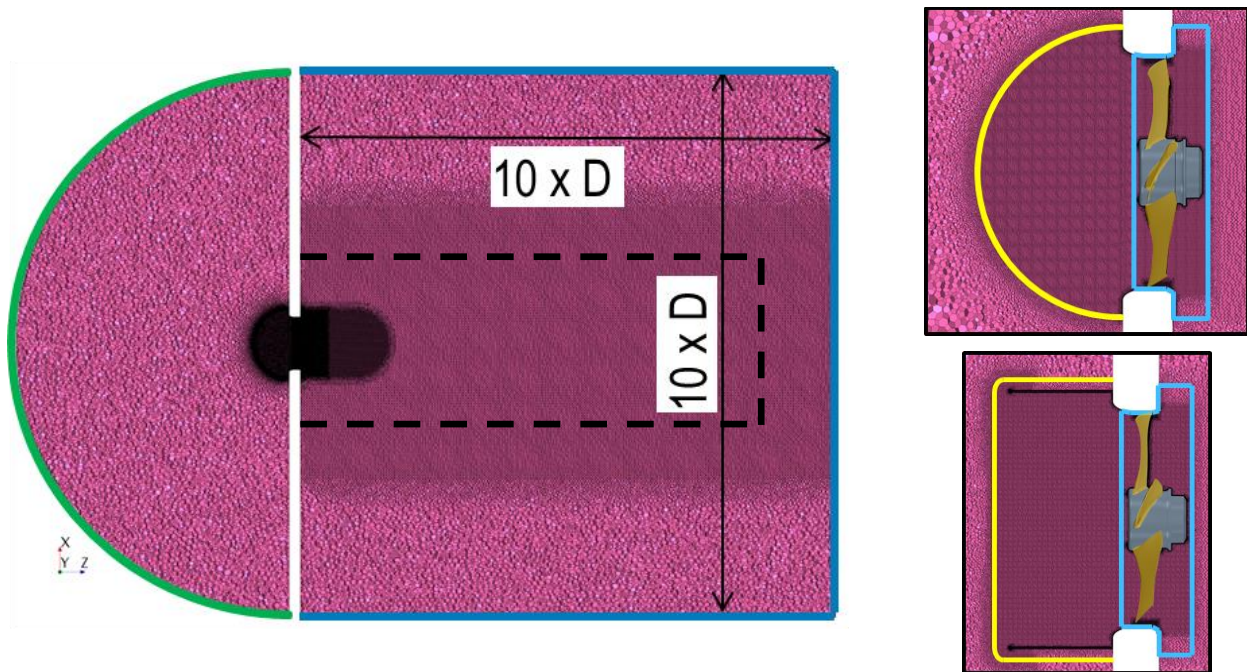


Figure 6: computational model, dimensions and permeable FW-H surface for both configurations

The inlet and outlet boundary conditions need to be non-reflective since the experiments were conducted in anechoic chamber. Free stream boundary condition was applied as inlet, which is non-reflective for waves normal to the boundary. The free stream boundary condition actually acts similar to a pressure boundary condition. For this reason mass flow rate is not fixed for the compressible LES simulation. The inlet pressure for free stream is taken from previous RANS with mass flow inlet and fixed pressure outlet. Since the LES result deviates from RANS a shift in flow rate appears. This could be fixed by adjusting the inlet pressure. In the present case the maximum deviation in flow rate was around 7 % in case of fan with box (figure 7), which is of acceptable accuracy. No further adjustment of inlet pressure was applied.

On the pressure side an acoustic suppression zone was used to damp out acoustic waves as well as turbulent structures before reaching the boundary. The size of the suppression zone was quite large as indicated in figure 6 with the dashed line. In preliminary simulations unphysical pressure fluctuations appeared on the pressure side. This spurious sound was found to increase the sound pressure spectra on the suction side of the fan. The location of this numerical source was located within the turbulent wake of the fan. The most effective way to remove these fluctuations was to increase the size of the suppression zone to include the source region. With increased size of the suppression zone still some spurious fluctuations appear on the pressure side, but with much less effect on the sound spectrum as will be shown later. This effect occurred only for the case with clean inflow, despite the fact that the mesh on the pressure side was of the same size and topology for both configurations. The mesh quality is very high, since in the wake volumetric controls are used to refine the mesh. This leads to very regular cells with constant size through the control region.

Simulation results

Figure 7 shows the aerodynamic performance of the time averaged LES compared to measurements. The total to static pressure rise in the LES computation is evaluated from the time averaged mean of pressure at the border of the sponge zone, and the time averaged mean of total pressure at inlet. LES pressure rise is higher than measured. Field variables inside the sponge zone should be used with care, since the result may not be physical. The idea of the sponge zone is to add mass sources or sinks where pressure field deviates from the reference solution. In this way pressure field is forced to the reference field at outlet

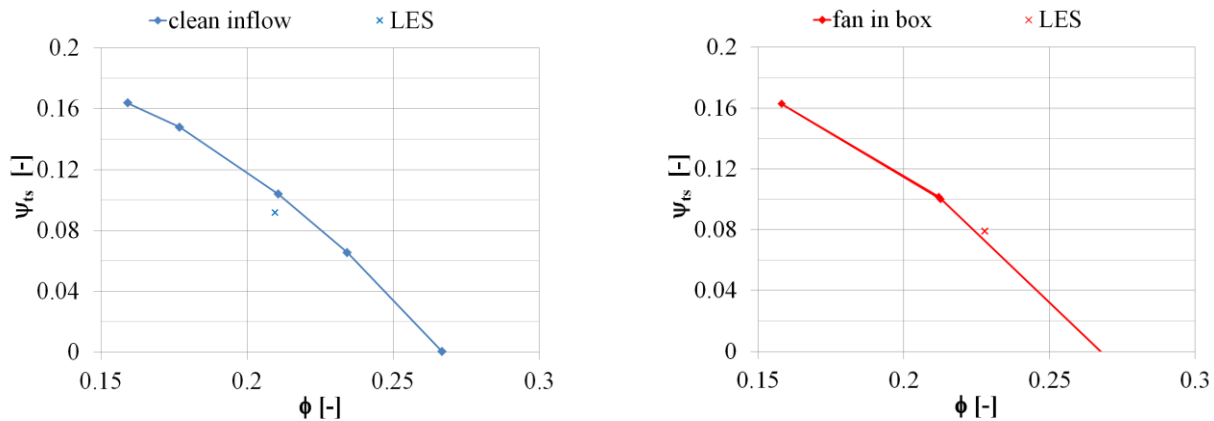


Figure 7: fan performance, simulation vs experiment

In the following section the predicted sound pressure spectra are compared to measurements. The frequency resolution was rather low in the simulations. Due to the large model size the CPU times are much higher compared to standard RANS simulations of such a setup. For that reason only 2 full revolutions were considered for acoustic evaluation and averaging the flow field. From an initial RANS solution 3 revolutions with larger time step were simulated to achieve a developed flow field. The resulting frequency resolution for simulation is 100 Hz. For that reason tonal noise is not resolved. A proper resolution of tonal noise in simulations with Δf 1/10 BPF would require at least 10 revolutions in order to achieve a minimum statistical average of 9 blocks at 50 % overlap. For a proper comparison measured spectra are in figure 8 shown with Δf 1 Hz and 100 Hz respectively.

The sound spectra show a good agreement to measurements up to 2 kHz (figure 8). In case of clean inflow a peak at 1200 Hz due to spurious noise is found. It is less pronounced for the microphone 8 off the axis of rotation. This effect is not visible for the FW-H propagation from the solid blades. The usage of permeable FW-H surface is much more sensitive to a polluted solution, since all fluctuations on the surface are assumed to be sound propagated to the far field. From 2 kHz to 4 kHz some broad band hump is found in the simulation for both configurations. This may be attributed to under resolved attached boundary layer on the blades. Both methods for calculating the far field sound pressure lead to very similar results. This is especially interesting for the case with box in front. The fact that free field propagation from the blades is identical to permeable FW-H propagation outside the box shows, that the box has only minor effect on the propagation to the far field. The permeable FW-H solution drops down at frequencies larger than 4.5 kHz, which is higher than expected. The vertical black solid line indicates the limit frequency of 3.0 kHz which was used to design the mesh. 20 cells per wave length shows to be conservative estimation, which is attributed to the 3rd order convection scheme. Despite the hump, the influence of the disturbed inflow was well predicted.

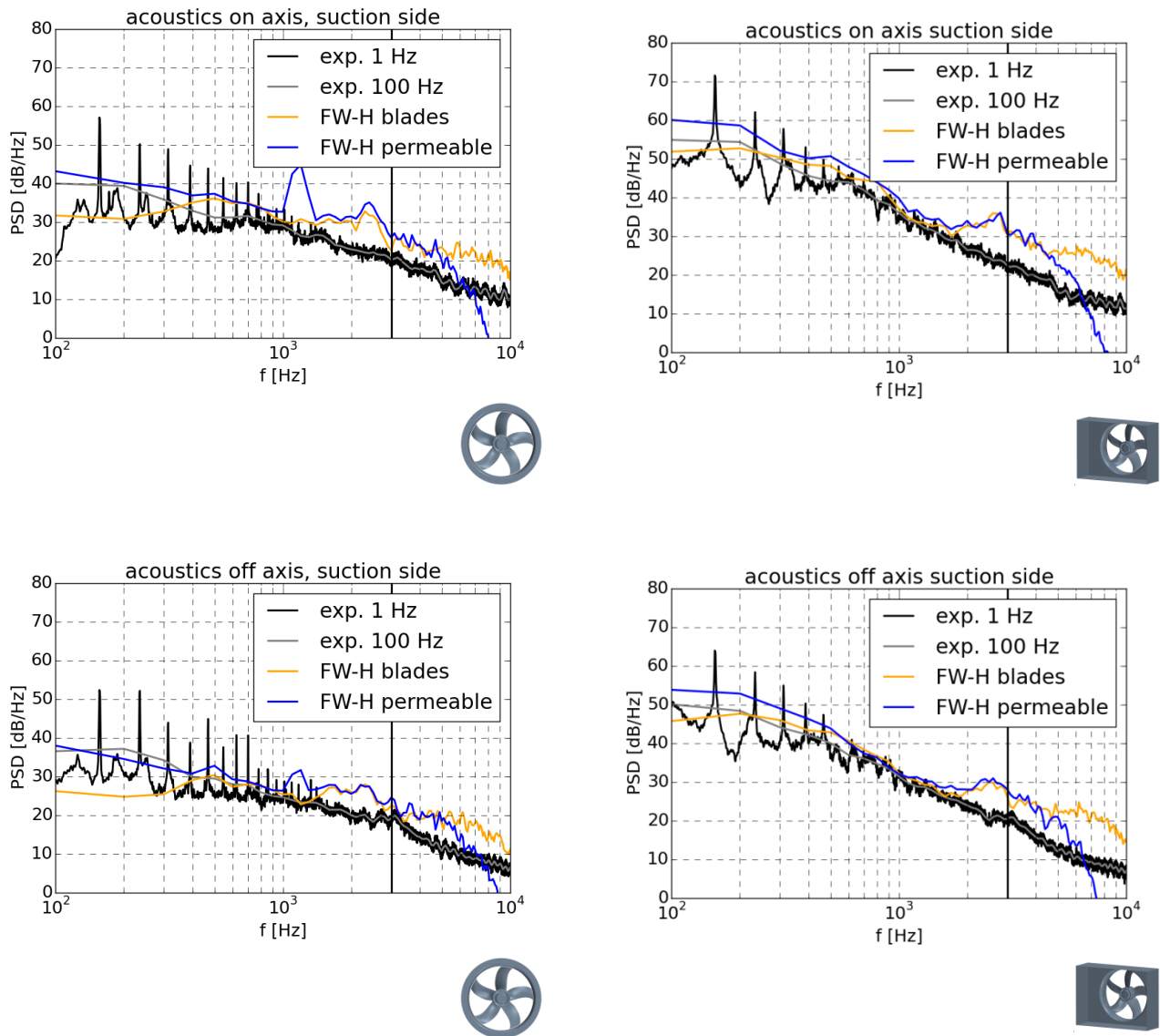


Figure 8: comparison of sound pressure spectra, (left) clean inflow, (right) fan in box, (top) on axis, (bottom) off axis

VISUALISATION OF FLOW FEATURES

The array measurements in stationary frame show stationary sources of sound. Detailed analysis of the flow features are shown in the following section.

The flow inside the box was visualised in terms of vorticity and velocity fields from time averaged LES results (figures 9 and 10). Vortical structures start from the corners of the box. There are two counter rotating vortices on each side of the bottom wall. In the middle of the box the vortices unite to a large region of high turbulent kinetic energy. This effect is most prominent on the bottom and top walls. On the side walls the local extension of this highly turbulent region is smaller due to the asymmetry of the rectangular box. The blades cut through this highly turbulent region, leading to increase of broadband as well as tonal noise of the fan.

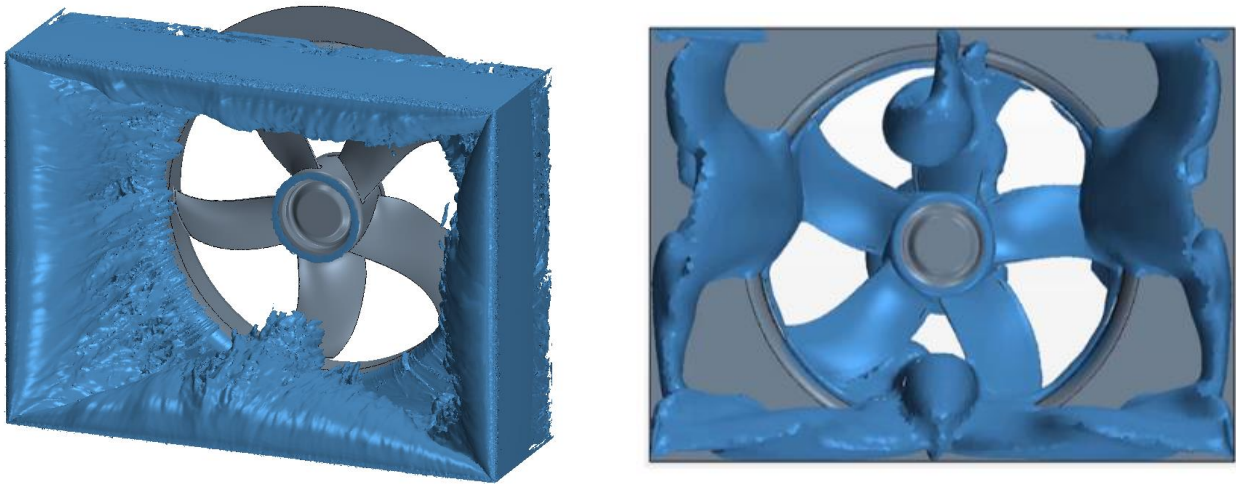


Figure 9: isosurface of LES mean vorticity and turbulent kinetic energy from URANS

For flow visualisation of kinetic energy URANS solution is shown. In LES the mean flow field is not developed in time during 2 rotor revolutions. Especially the turbulent inflow inside the box fluctuates with low frequencies, so that much more physical simulation time would be needed to achieve steady mean flow.

In experiments several methods are known for flow visualisation. In this case a very simple and cheap technique for visualisation of near wall velocity or wall shear stresses respectively was applied, in order to show flow separation. A mixture of ethyl alcohol and talcum powder was spread on the bottom wall of the box. If a thin layer of the mixture is exposed to fluid flow on a solid surface, the ethyl alcohol evaporates quickly. The talcum is convected with fluid velocity and sticks on the surface if the surrounding ethyl alcohol is evaporated. The powder arranges along the fluid streamlines, resulting in a visualisation of the near wall velocity field. In order to increase the contrast the bottom wall of the box was painted in matt black. A limitation of the method is that it can only be applied to horizontal plain or weakly curved surfaces. On inclined or curved surfaces the mixture itself will start to flow. In such a case it is not possible to visualise the primary flow independently.

Figure 10 displays the result of the flow visualisation. The left picture depicts a detailed inspection of the LES mean velocity field. The flow field in the box is very complex with a main vortical structure coming from the box corner. This feature could also be found in experimental flow visualisation. The talcum powder nicely shows the trace of vortical structures coming from the corners. In the middle of the plate the trace has changed to main flow direction. Size as well as trace of the corner vortex is in good agreement between simulation and experimental flow visualisation.

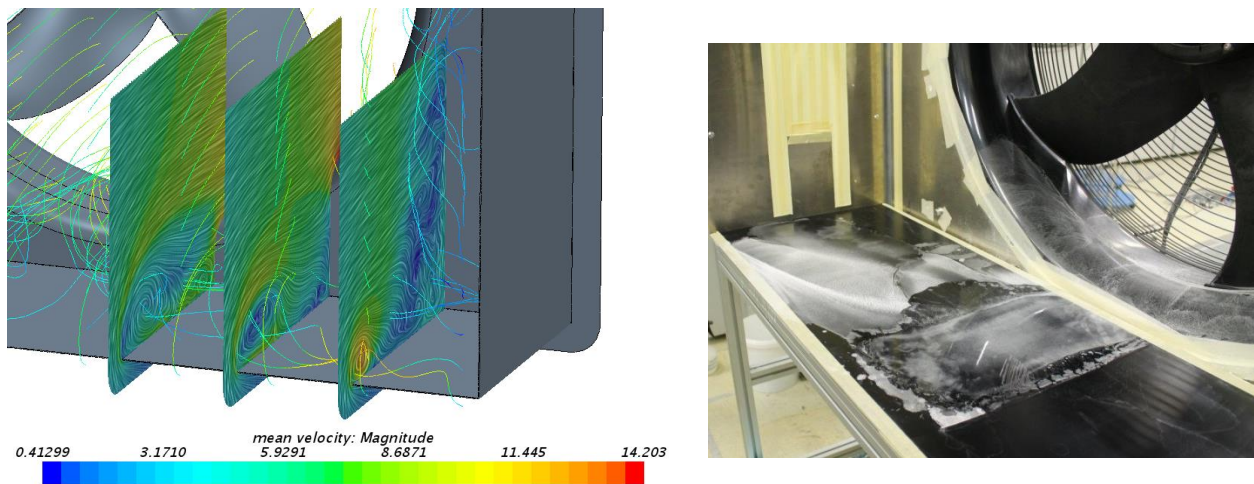


Figure 10: flow visualisation on the bottom wall of the box, left LES mean velocity, right experiment

CONCLUSION

The rectangular box as simplified configuration of customer application has been shown to dramatically increase sound pressure. The reason is the separation of corner vortices from the sharp edges of the box. These vortices unite to large regions of high turbulence in the middle of the bottom and top walls of the box. The difference of sound spectra due to inflow disturbance was well predicted by an LES within the limitation of industrial feasibility.

In addition to simulation further evidence of the sound generation mechanism was given by array measurements and experimental flow visualisation. For disturbed inflow sound sources move from the blade tip and trailing edge to the leading edge, which is typical for turbulence ingestion noise. Sources appear at outer radial positions. The evaluation of sound sources in stationary frame showed steady sources at four locations near the middle of each wall of the box. Strong sources appear at bottom and top wall and weaker sources at the side walls. The flow visualisation on the bottom box supplements the findings. Traces of the corner vortices are found which match excellently with LES wall shear results.

BIBLIOGRAPHY

- [1] T. Carolus *Ventilatoren*, Springer Vieweg **2012**
- [2] F. Zenger, M. Becher, S. Becker - *Influence of inflow turbulence on aeroacoustic noise of low speed axial fans with skewed and unskewed blades*, Fan 2015 Conference, Lyon, **2015**
- [3] ISO 5801 – *Industrial fans – Performance testing using standardized airways*, **2010**
- [4] ISO 13347-3 *Industrial fans – Determination of fan sound power levels under standardized laboratory conditions – part 3: Enveloping surface method*, **2006**
- [5] G. Herold, E. Sarradj - *Microphone array method for the characterization of rotating sound sources in axial fans* Noise Control Engr. J. 63 (6), November-December **2015**
- [6] F. Zenger, G. Herold, S. Becker - *Acoustic Characterization of Forward- and Backward-Skewed Axial Fans under Increased Inflow Turbulence* Proceedings of the 22nd AIAA/CEAS Aeroacoustics Conference, Lyon, France, **2016**

- [7] P. Sijtsma - *CLEAN based on spatial source coherence* International Journal of Aeroacoustics, 6(4), **2007**
- [8] C. A. Wagner, T. Hüttl, P. Sagaut – *Large-Edy Simulation for Acoustics*, Cambridge University Press, **2007**
- [9] STAR-CCM+® Documentation Version 11.02, **2016**
- [10] K. S. Brentner, F. Farassat - *Analytical Comparison of the Acoustic Analogy and Kirchoff Formulation for Moving Surfaces* AIAA Journal, Vol. 36, No.8, **1998**